Self-Similarity Properties of the Probability Distribution Function of Turbulence-Induced Particle Fluxes at the Plasma Edge

B. A. Carreras
Oak Ridge National Laboratory, Oak Ridge, Tennessee 37831-8070

B. van Milligen, C. Hidalgo, R. Balbin, E. Sanchez, I. Garcia-Cortes, and M. A. Pedrosa
Asociación Euratom-Ciemat, 28040 Madrid, Spain

J. Bleuel and M. Endler
Max-Planck-Institut für Plasmaphysik, Euratom Association, 85740 Garching, Germany
(Received 2 June 1999)

The probability distribution function of the turbulence-induced particle flux at the plasma edge has distinct functional forms over two distinct ranges of time scales. One range corresponds to the fluctuation time scales and the other one is the mesoscale range: time scales between the turbulence decorrelation and confinement time. In the second range, the probability distribution function is self-similar and essentially has only the outward flux tail. This structure reflects some of the mechanisms of the underlying turbulence.

PACS numbers: 52.35.Ra, 52.55.–s

From the Langmuir probe measurements in low-power Ohmically heated or electron cyclotron heated plasma discharges and for several types of confinement devices, we have concluded that the electrostatic potential and density fluctuations at the plasma edge are self-similar over a broad range of time scales [1,2]. The self-similarity range is, in general, for time scales longer than the turbulence decorrelation times up to times of the order of confinement time, the mesoscale range. The upper bound of the self-similarity range is difficult to determine because of the lengths of time records available and the varying plasma conditions on these longer time scales. It was found that for fluctuation measurements within the plasma confinement region the self-similarity parameter [3] varies between $H = 0.62$ and $H = 0.75$, a relatively small range of variation given the diversity of plasma confinement devices considered.

To find out whether these properties of the plasma fluctuations have any bearing on the dynamics of plasma transport, we must investigate the properties of their induced fluxes. The relative phase between density and potential fluctuations could be such that the induced particle flux does not share the self-similarity properties. The problem with studying fluxes is the scarcity of experimental measurements. Flux measurements for core plasmas are practically nonexistent. At the plasma edge, the turbulence-induced particle flux can be inferred from the simultaneous measurement of the density and potential fluctuations. By measuring the density fluctuations at one point in the plasma, $\tilde{n}_1 = \tilde{n}(r_1, \theta_1, t)$, and the electrostatic plasma potential at two nearby positions, $\phi_1 = \tilde{\phi}_2(r_1, \theta_1 - \delta, t)$ and $\phi_2 = \tilde{\phi}_3(r_1, \theta_1 + \delta, t)$, the instantaneous turbulence-induced particle flux at this location can be calculated, $\Gamma_t = \tilde{n}\tilde{E}_\theta/B = \tilde{n}_1(\phi_2 - \phi_1)/(2r_1\delta B)$. Here, B is the magnetic field and E_θ is the poloidal electric field. Of course, what the Langmuir probe measures is the ion saturation current, $I_S \propto n\sqrt{T_e}$, and the floating potential, $V_f = \Phi - 3T_e$. Therefore, the flux inferred from these measurements is not necessarily equal to the particle flux. However, measurements of the temperature fluctuations at the plasma edge in some confinement devices have shown that their relative phase is such that Γ_t calculated from I_S and V_f is a good estimate of the particle flux [4,5].

One of the main results of the present analysis is that the self-similarity of the electrostatic potential and density fluctuations translates into self-similarity of the turbulence-induced fluxes. The value of the self-similarity parameter for the turbulence-induced particle fluxes is close to the corresponding value for the fluctuations and is significantly distinct from and greater than $H = 0.5$. This indicates that the autocorrelation function of the fluxes decays algebraically for long time lags. The self-similarity of the fluxes implies that their probability distribution function (PDF) scales in a well-defined way when we change the time scale over which the flux is calculated. To be more precise, let us consider a time sequence of measured fluxes $F \equiv \{\Gamma_t; t = 1, \ldots, N\}$. Here, Γ_t is the flux at time t and N the total number of data points in the record. We can now construct time records with a temporal resolution m, $F^{(m)} = \{\Gamma_\tau^{(m)}; \tau = 1, \ldots, N/m\}$, by averaging over nonoverlapping blocks of m elements from the original series F. That is, we define the following averaged fluxes:

$$\Gamma_t^{(m)} = \frac{1}{m} \sum_{i=1}^{m} \Gamma_{mt-m+i} \,. \tag{1}$$

The meaning of the $F^{(m)}$ series is clear; it is the series of the measured fluxes over a time scale that is m times longer than the original time scale. In the time range in which the fluctuations are self-similar, the PDF, $P(\Gamma)$, of the fluxes scales as

$$P(\Gamma^{(m)}) = m^{H-1} g\left(\frac{\Gamma^{(m)} - \langle\Gamma\rangle}{m^{H-1}}\right), \qquad (2)$$

where g is a universal function and $\langle\Gamma\rangle$ is the averaged flux. This relation results from the assumption of self-similarity and the condition that the value of the integrated probability over all $\Gamma^{(m)}$ is 1. Equation (2) is a strong constraint on the distribution of fluxes. However, the self-similarity of the fluctuations and fluxes does not provide any information on the functional form of g. We must determine g from a dynamical theory or from the experimental measurements.

From the analysis of experimental data, we have found that the PDF of fluxes is self-similar over a wide range of time scale. In Fig. 1, we have plotted the standard deviation $\sigma(m)$ for each of the $F^{(m)}$ series derived from the induced particle flux data obtained from a discharge in the W7-AS device. The self-similarity ranges are the regions in m in which $\sigma(m) \propto m^{H-1}$. For a range of time scales around the fluctuation decorrelation time, $1 \leq t \leq 30$ μs, the fluxes seem to be self-similar with a self-similarity parameter close to 1, $H = 0.85$. We will refer to this range of time scales as the fluctuation range. However, this range of time scales is relatively short and $\sigma(m)$ may not be just a simple power function. Therefore, it is not possible to claim strict self-similarity in this range of scales. The situation is clearly different for time scales longer than 60 μs, the mesoscale range. In this case, the self-similarity range is well defined at least over three decades and the self-similarity parameter $H = 0.58$. The precise value of the self-similarity parameter varies with the confinement device and plasma conditions, but their range of variation is narrow. This self-similarity range corresponds to the one discussed in Ref. [2] for the density and electrostatic potential fluctuations. Here, we use as fluctuation decorrelation time the value of the time lag at which the autocorrelation function has decreased by e^{-1}. For W7-AS plasma edge data, this value is about 10 μs. The mesoscale range is defined as the time scales between 5 times the decorrelation time and the particle confinement time.

In this paper, we use plasma edge fluctuation measurements only from the W7-AS device [6]. The reason is that we need both three-point probe measurements and long time records. These constraints preclude the use of much of the fluctuation data available. To have long time records within the plasma edge region, it also implies the use of data mostly around and within the shear flow layer. Because of this, the averaged value of the self-similarity parameter is about 0.6. For these data sets, we have calculated the PDF of the fluxes over the two time scale ranges. The original time records are about 100 000 points with a sampling rate of 1 MHz. In the calculation of the PDFs, we change the time resolution by factors of 2. In this way, the largest scale that we can investigate is up to 1.024 ms. We cannot go to time resolution above this value because there are not enough points left after averaging to calculate a PDF. For these data, we can separate the time scales into two ranges: the ones in $1 \leq m \leq 32$ as the fluctuation range, and the time scales in $64 \leq m \leq 1024$ as the mesoscale range (Fig. 1). Although a true self-similarity of fluctuations and fluxes is questionable in the fluctuation range, we have used the rescaling of the PDF, Eq. (2), to illustrate its functional form in this range (Fig. 2). The rescaled PDFs calculated in the mesoscale self-similarity range are shown in Fig. 3. Because the averaged flux has

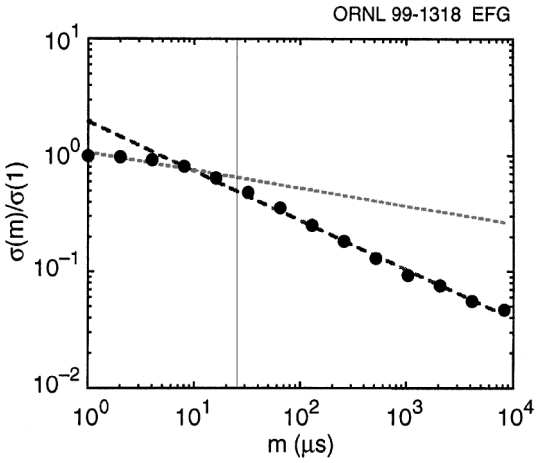

FIG. 1. Standard deviation for each of the series $F^{(m)}$ derived from the induced particle flux as a function of m. The data are from discharge number 35427 in the W7-AS device.

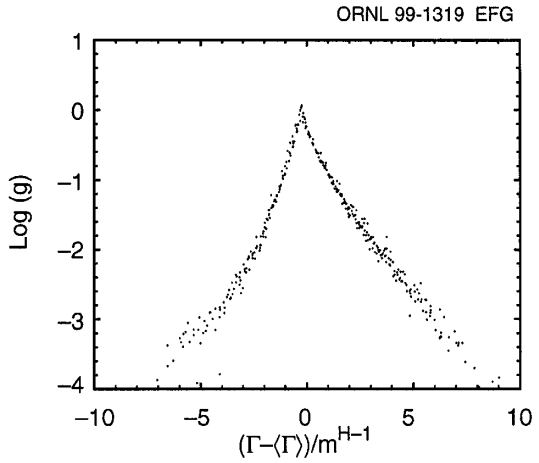

FIG. 2. Probability distribution function of the turbulence-induced fluxes for time scales in the range $1 < m < 32$. The data are from discharge number 35427 in W7-AS.

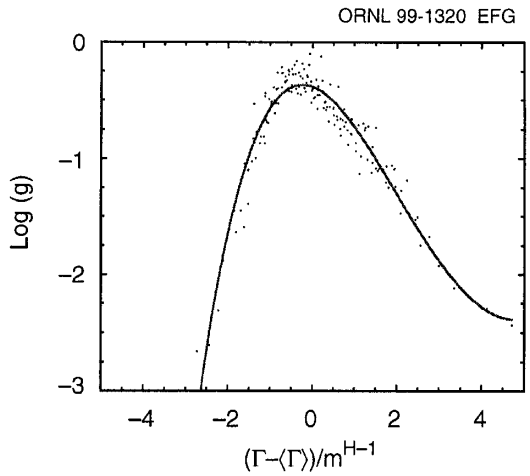

FIG. 3. Probability distribution function of the turbulence-induced fluxes for time scales in the range of $64 < m < 1024$. The data are from discharge number 35427 in W7-AS.

been subtracted before the rescaling, the peak of the PDFs in both figures is slightly shifted towards the negative values of the x axis.

In Fig. 2, we have plotted six realizations of the PDF of fluxes corresponding to rescaled time by powers of 0 to 5. They have been rescaled in the form indicated by Eq. (2). The six realizations fall on top of each other, showing an approximate form of self-similarity of the PDF. The functional form of this PDF is the same as the one that has been calculated for different devices and plasma conditions [7,8]. It has a long positive tail (transport out of the plasma) but also a negative tail (transport into the plasma). The tail falls off slowly. For the case of the DIII-D tokamak, it has been determined that $P(\Gamma) \propto \Gamma^{-1}$ for large Γ [8]. A considerable fraction of the transport out of the plasma is caused by the large tail transport events (10% of the largest transport events are responsible for 50% of the transport) [9].

The rescaled PDF for the mesoscale self-similarity range has been plotted in Fig. 3. We have used five realizations of the PDF for powers of 2 from 64 to 1024. The PDFs, once rescaled, fall again on top of each other. In this range, the functional form of the PDF is clearly different from the one in Fig. 2. The falloff index of the positive flux tail remains very similar to the case of short scales, but the negative flux tail practically disappears. Since the statistics decrease with the increase in the time scale, it is difficult to determine how fast the falloff of the positive tail is. However, there is no doubt of the sharp suppression of the negative tail. The distribution of the small fluxes also changes.

A way of quantifying the differences between the two forms of the PDF is by calculating the integral over the positive and negative fluxes, $I_+ = \int_0^\infty P(\Gamma)\, d\Gamma$ and $I_- = \int_{-\infty}^0 P(\Gamma)\, d\Gamma$. The difference between these two integrals is a measure of the asymmetry of the PDF, which we define as $A = I_+ - I_-$. For all cases considered and because the data are around the shear flow layer, the asymmetry of the fluxes in the fluctuation range is rather low, $A = 0.25 \pm 0.07$. However, it is close to 1, $A = 0.85 \pm 0.07$, in the mesoscale self-similarity range. The distribution of values of A for all of the discharges considered is shown in Fig. 4. When we analyzed the few data sets available within the plasma edge but separated from the shear flow layer, the value of A in the fluctuation range is somewhat higher, $A > 0.3$, but it does not change significantly in the mesoscale range.

These experimental results can be interpreted with a simple picture for the turbulence mechanism. Basically we may consider two types of mechanisms in operation. One mechanism is the usual eddy transport associated with plasma instabilities. These eddies have an average size of the order of the correlation length (about 1 cm in the plasma edge) and a characteristic lifetime of the order of a turnover time (about 10 μs in these plasmas). These eddies create fluxes of particles in and out of the plasma with a dominant outward effect because of the averaged density gradients. If we assume that the distributions of the poloidal electric field and of the density fluctuations are Gaussian distributions, but there is some level of cross correlation, γ, between them, the PDF of the induced fluxes [9] is

$$P(\Gamma) = \frac{1}{\pi} \frac{\sqrt{1-\gamma^2}}{\bar{n}\bar{E}_\theta} K_0\left(\frac{|\Gamma|}{\bar{n}\bar{E}_\theta}\right) \exp\left(\gamma \frac{\Gamma}{\bar{n}\bar{E}_\theta}\right). \quad (3)$$

Here K_0 is the modified Bessel function, $\bar{n}$ is the rms value of the density fluctuations, and $\bar{E}_\theta$ is the rms value of the poloidal electric field fluctuations. The level of coherence controls the in and out asymmetry of the fluxes. This functional form well describes the region of small fluxes of the distribution in Fig. 2, but does not describe the large $|\Gamma|$ tails.

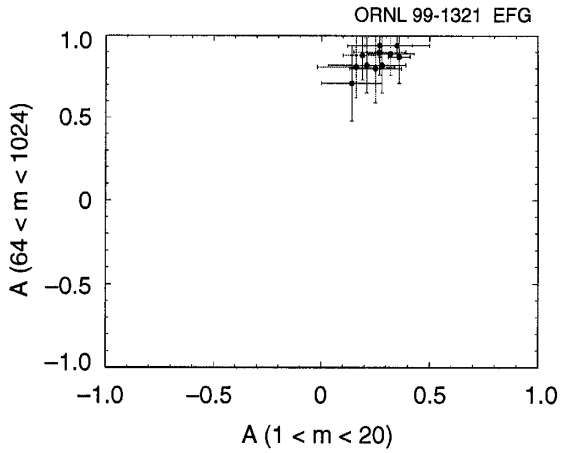

FIG. 4. Distribution of values of the asymmetry of the flux PDF in the two self-similarity regions.

A second mechanism is linked to flux pulses. They correspond to time scales in the mesoscale range and are responsible for the large tail of positive fluxes. One possible interpretation is an avalanchelike process. The eddy-induced transport in one radial position changes the gradient of the average profile (or the averaged profile scale length) in its immediate radial vicinity, triggering instabilities in the neighboring points. This type of phenomenon creates a coherent sequence of fluxes, that is, an avalanche. These avalanches are of all sizes and they move mostly outward. Note that although models based on self-organized criticality (SOC) [10] show that the avalanches propagate in both directions, the density of particles moves out and holes move in. Therefore, the particle flux is only outwards.

There are other possible explanations for these large flux pulses. An alternative one is the creation of fluctuation bursts in the proximity of the plasma edge shear flow layer due to a near balance between fluctuation drive and shear flow stabilization effects. Analysis is under way to distinguish between these two mechanisms.

In the fluctuation scale range, Fig. 2, the PDF of the flux captures both types of transport events. We can see the near symmetric structure of the PDF associated with the direct effect of the local eddies, but we cannot see the accumulative effect of fluxes leading to an avalanche. However, in the mesoscale range, we have averaged over the eddy time scales and only the long time transport events remain. They essentially cause outward transport. They have a dominant effect on the overall transport, and on the cross-power spectral function [11] between the density fluctuations and potential component of the electric field fluctuations peaks in this range of time scales. It is also interesting to note that this range of time scales overlaps with the frequency range in which the power spectrum of fluctuations is close to $1/f$ in the plasma frame [12].

Transport by avalanches may be consistent with plasma transport models based on the concept of self-organized criticality [10]. It has been suggested that the SOC approach should be used to understand plasma transport [13,14]. There is some indirect experimental evidence for SOC behavior of magnetically confined plasmas in the so-called low confinement regime. Phenomena such as the resilience of plasma profiles to changes in the location of the heating source, Bohm scaling of the diffusivities, and the apparent nonlocal behavior of some perturbative experiments could be consequences of SOC. To this evidence, we may now add the existence of long-range correlation in plasma fluctuations [1] and the existence of a $1/f$ frequency range in the spectrum [8,12]. The analysis of fluxes, such as the one presented here, complements those studies and should enable one to get closer to understanding the dynamics of plasma transport.

This research was sponsored in part by Dirección General de Investigaciones Científicas y Técnicas of Spain under Project No. PB96-0112-C02-02 and by Oak Ridge National Laboratory, managed by Lockheed Martin Energy Research Corporation for the U.S. Department of Energy under Contract No. DE-AC05-96OR22464. We also want to acknowledge the Joint Commission for Scientific and Technological Cooperation between the United States and Spain for their support during the completion of this research.

[1] B. A. Carreras *et al.,* Phys. Rev. Lett. **80**, 4438 (1998).
[2] B. A. Carreras *et al.,* Phys. Plasmas **5**, 3632 (1998).
[3] G. Samorodnitsky and M. S. Taqqu, *Stable Non-Gaussian Random Processes: Stochastic Models with Infinite Variance* (Chapman and Hall, New York, 1994).
[4] H. Lin, R. D. Bengtson, and C. Ritz, Phys. Fluids B **1**, 2027 (1989).
[5] C. Hidalgo *et al.,* Phys. Rev. Lett. **69**, 1205 (1992).
[6] J. Bleuel *et al.,* in *Controlled Fusion and Plasma Physics* (European Physical Society, Kiev, 1996), Vol. 20C, p. 727.
[7] M. Endler *et al.,* Nucl. Fusion **35**, 1307 (1995).
[8] T. L. Rhodes *et al.,* Phys. Lett. A **253**, 181 (1999).
[9] B. A. Carreras *et al.,* Phys. Plasmas **3**, 2664 (1996).
[10] P. Bak, C. Tang, and K. Wiesenfeld, Phys. Rev. Lett. **59**, 381 (1987).
[11] E. J. Powers, Nucl. Fusion **14**, 749 (1974).
[12] B. A. Carreras *et al.,* Phys. Plasmas (to be published).
[13] P. H. Diamond and T. S. Hahm, Phys. Plasmas **2**, 3640 (1995).
[14] D. E. Newman *et al.,* Phys. Plasmas **3**, 1858 (1996).